PAPER • **OPEN ACCESS**

PZT actuators as on-board instruments to reduce vibrations and strains in submerged structures

To cite this article: X Sánchez-Botello *et al* 2022 *IOP Conf. Ser.: Earth Environ. Sci.* **1079** 012097

View the article online for updates and enhancements.

You may also like

- Development of an optically modulated piezoelectric sensor/actuator based on titanium oxide phthalocyanine thin film
Kuan-Ting Chen, Shiu-Duo Huang, Ying-Heng Chien et al.
- Topological design of compliant smart structures with embedded movable actuators
Yiqiang Wang, Zhen Luo, Xiaopeng Zhang et al.
- Time delay control of hysteretic composite plate
Long-Xiang Chen, Shi-Hong Li, Kun Liu et al.

244th Electrochemical Society Meeting
October 8 – 12, 2023 • Gothenburg, Sweden
50 symposia in electrochemistry & solid state science
Abstract submission deadline:
April 7, 2023
Read the call for papers &
submit your abstract!

This content was downloaded from IP address 147.83.76.238 on 15/02/2023 at 08:28

PZT actuators as on-board instruments to reduce vibrations and strains in submerged structures

X Sánchez-Botello[1], O de la Torre[1], R Roig[1], R Costa-Castelló[2] and X Escaler[1*]

[1] Barcelona Fluids & Energy Lab, Universitat Politècnica de Catalunya, Barcelona, Spain
[2] Institut de Robòtica i Informàtica Industrial, Universitat Politècnica de Catalunya, Barcelona, Spain.

*xavier.escaler@upc.edu

Abstract. This paper presents the design and evaluation of an active control system to reduce vibrations and strains of submerged structures. For that, a metallic disk mounted in a test rig has been equipped with on-board waterproof strain gauges and accelerometers, to measure its structural response, and with an on-board PZT actuator patch, to provide the required control force. This control force is computed in real-time by an optimal algorithm that determines the exact voltage to be supplied to the PZT patch in order to mitigate any increase of vibrations and/or strains detected by the sensors. In order to capture the dynamics of the structure when it is excited both in air and submerged in water, a plant model has been identified from the Frequency Response Functions (FRFs) obtained experimentally from the measured vibrations and numerically from simulated strains. With these plant models, two different control techniques based on a Linear Quadratic Gaussian (LQG) controller and on an H_∞ controller have been implemented and simulated under different types of excitations. The obtained results are satisfactory and support the need to continue the research to validate them experimentally.

1. Introduction

Hydraulic turbines are complex structures partially submerged in water which are submitted to unsteady forces during transient and off-design operations. As a result of the hydraulic phenomena produced at those conditions, these machines are prone to suffer vibrations that can cause a reduction of their performance and live cycle duration. As a part of the H2020 EU-funded AFC4Hydro project [1], a Structural Health Monitoring (SHM) system combined with an active controller is under development, which aims to optimize the turbine structural response and improve its performance by acting on the draft tube flow. The worst-case scenario can occur when the frequency of a given excitation is equal to one natural frequency of the structure, causing a resonance. Under resonance conditions, the amplitude of the induced vibrations will increase and, if sustained in time, they might provoke fatigue cracks and a catastrophic failure.

In order to mitigate the structural vibrations and improve the structural functionality and safety, different control systems have been traditionally applied, typically classified into passive, semi-active, active and hybrid control systems [2]. A passive control system reduces the vibration by dissipating the energy of the system without adding to it any external power, solely using dissipative devices such as damping materials, viscoelastic or frictional dampers and vibration absorbers. Although these passive methods are simple, cheap and always stabilize the system, due to being energy dissipators, they may

Content from this work may be used under the terms of the Creative Commons Attribution 3.0 licence. Any further distribution of this work must maintain attribution to the author(s) and the title of the work, journal citation and DOI.
Published under licence by IOP Publishing Ltd

not be effective when the operating conditions change, since they have a fixed design. In addition, passive methods are mainly used to reduce high-frequency vibrations or narrow frequency bands, but they often have poor performance for low-frequency responses [3].

Active, semi-active and hybrid control systems are generally based on feedback or feedforward control schemes that suppress the vibration of the structure at any operating condition by producing a force calculated according to the real-time information collected by the sensors. A typical active control system consists of a plant, actuators, sensors and control electronics. The vibration control is then achieved by applying a secondary input to the structure, thereby modifying the dynamic response of the system to a desirable pattern [4]. While active systems are generally more effective than passive ones, they have the disadvantages of being complicated and expensive, having the potential to destabilize the system, and being sensitive to system modeling errors and uncertainties.

The present work is focused on developing a methodology to design an active control system to reduce the vibrations and enhance the integrity of a simple submerged structure. This active control system will measure in real-time the signals coming from different on-board sensors, placed on the surface, and compute the control force needed to be applied by means of a PZT patch. Similar to the work of Kamel et al. [5], the control algorithm programmed in MATLAB® has been designed based on a state-space model calculated using identification tools from the Frequency Response Function (FRF) of the system. Thus, the controller is designed based on the plant model of the system, which is obtained mathematically using identification techniques from the FRFs of the system because deriving a mathematical model involving the different physical phenomena taking place is too complicated [6]. Although the FRFs for the strains have been obtained with numerical modal analysis performed in ANSYS®, the FRFs for the vibrations have been obtained with an experimental modal analysis in the laboratory test rig. From the obtained state-space models, two controllers have been designed and implemented to reduce the strains/vibrations of the structure in air or submerged in water, which are a Linear Quadratic Gaussian (LQG) and an H_∞ controller. Compared with other traditional controllers such as the PIDs mainly used in industrial fields, these two proposed control schemes are more robust in terms of parameter uncertainty and disturbances, in addition to being optimal and thus providing robust stability with a minimized energy-like performance index [7].

Even though the present work is only centered on the theoretical design and validation of the controllers, the next step would be to test them experimentally and use the PZT patch with the control algorithm to reduce the strain and vibrations of the structure on the test rig, as carried out for a cantilever beam by Zheng et al. [8].

2. Methodology for the design of the controllers

The active control system aims to reduce the strains and vibrations in a metallic disk placed on a test rig, which has been built by the Barcelona Fluids & Energy Lab (IFLUIDS) research group from UPC. As Figure 1 shows, the test rig includes a tank of water to submerge the disk in water and study the added mass effects of the surrounding fluid.

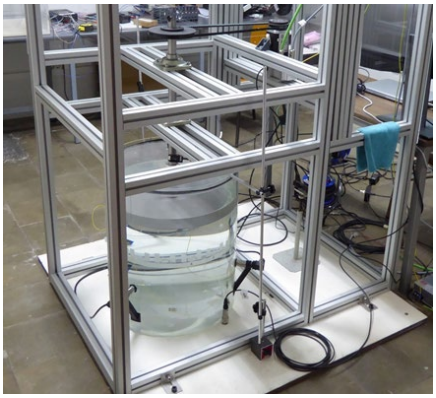

Figure 1. Test rig mounted in the laboratory to implement the active control method.

The disk is equipped with on-board waterproof strain gauges and accelerometers to measure the strain and vibration levels in different points. To obtain the FRFs for accelerations, an experimental methodology has been applied consisting in sending a voltage chirp signal to the PZT patch and measuring the vibrations. A chirp signal is a frequency-varying sinusoidal signal that sweeps between different frequencies with a constant amplitude, being able to excite different mode shapes. For the strains, a numerical model has been used based on an acoustic-structural simulation with the finite element software ANSYS® to obtain the strain levels measured at the strain gauge locations when a harmonic excitation is generated with the PZT patch. From each FRF, a model has been identified using MATLAB® in a limited frequency range where some modes of vibration exist. As the outputs obtained from the plants could be either accelerations or strains, the control objective of the controller has been to minimize them. Figure 2 shows graphically the workflow of the procedure followed in the present work to design, build and test the controllers for the disk in air and in water.

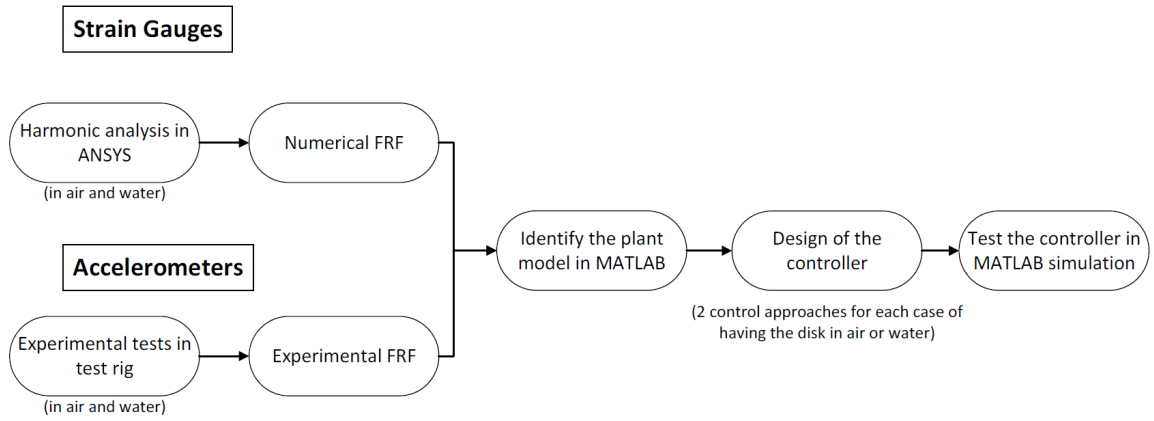

Figure 2. General workflow of the procedure to design and test the controllers.

2.1. Control approach 1. LQG controller (LQR+observer)

The first control approach implemented is a Linear Quadratic Gaussian (LQG) controller, which is a Linear Quadratic Regulator (LQR) controller combined with a Kalman filter. On the one hand, the LQR computes an optimal state-feedback control law $u = -Kx$ that minimizes a cost function $J(u, x)$, containing the weighting matrices Q and R that normalize and penalize the performance and effort, respectively. On the other hand, as it is not possible to measure all the states x of a model at each time instant, a Luenberger observer has been implemented using a Kalman filter to estimate all the states $\hat{x}$ from the measured output y_1 of the system, which can be either acceleration or strain. For the design of the Kalman filter, different uncorrelated 0-mean gaussian noise with constant power S_w and S_v have also been estimated from the real system to optimize the designed observer [9]. By using this controller, the control specifications are shaped in the temporal domain by tuning the different parameters, which are used to minimize the power of the vibration considering the amount of energy spent.

The LQG control has been implemented in the MATLAB®-based Simulink program following the scheme shown in Figure 3, where the measured output y_1 to be controlled is fed back using the computed LQG gain to obtain the control action of the PZT patch to minimize the vibration entering into the system. The excitation of the system is simulated as a sinusoidal disturbance signal of the same frequency as the natural frequency of the mode of vibration under consideration that lasts 2 seconds.

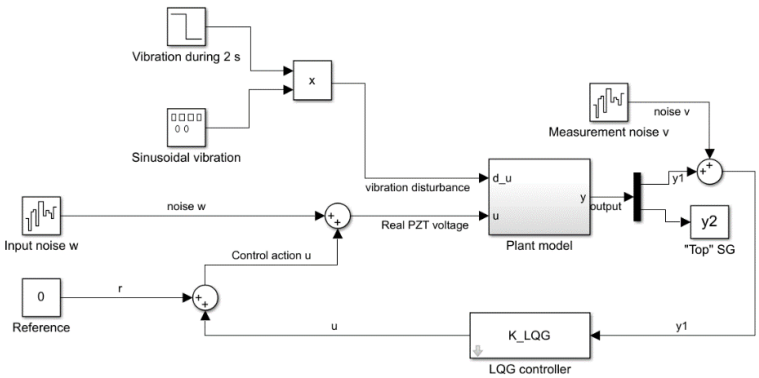

Figure 3. Control scheme of the LQG implementation in the Simulink® program.

2.2. Control approach 2. H_∞ controller

The second control approach is the H_∞ optimal controller, in which the closed-loop system has to be defined using the general control problem formulation (GCPF) presented in Figure 4. As it is shown, the GCPF distinguishes from the generalized plant P the exogenous inputs of the system w (in this case the vibration disturbance at the natural frequency) from the inputs of the plant u (the voltage of the PZT patch). Regarding the outputs of the generalized plant P, they have to be expressed as the sensed outputs v that are fed back to the controller (corresponding to the negative unitary feedback) and the exogenous outputs z to be minimized with respect to the inputs w (the amplitude of the vibration measured by the sensors, which can be either strain or acceleration) [10].

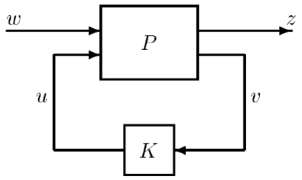

Figure 4. General control configuration [10].

Then, the H_∞ optimal control will find a controller K such that the closed loop system with the generalized plant P is stable and the H_∞ norm of the generalized plant P is minimized. The H_∞ norm shows how large the system's frequency response is across the frequency range, so it provides a measure of the largest factor by which any disturbance is magnified by the system. To design this controller, different weighting transfer functions can be introduced to shape the outputs z over frequency. Hence, differently from the previous LQG controller, in this case the control specifications are defined in the frequency domain, finding a trade-off between different objectives in various frequency ranges [11].

The Simulink® scheme of the implementation of this second control approach is presented in Figure 5, where the vibration of the system at resonance is introduced in the simulation as a plant disturbance lasting 2 seconds and vibrating at a natural frequency.

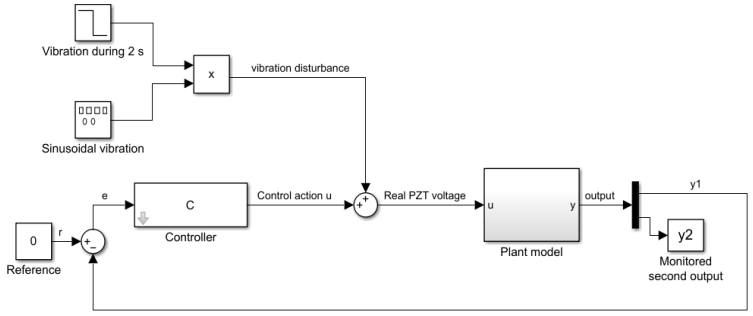

Figure 5. Control scheme of the H_∞ controller implementation in the Simulink® program.

3. Experimental setup

The experimental setup installed on the test rig to obtain the experimental FRFs of the disk in air and in water consisted of a computer connected to a NI cDAQ-9185 chassis with modules NI-9231 and NI-9235 to digitalize the sensor signals and to record them in binary format. The on-board sensors glued on the disk were two strain gauges and two accelerometers, named "Next" and "Top" for the strain gauges and "Acc_1" and "Acc_2" for the accelerometers. The strain gauges were the single-axis WFLA-3-17-3LDBTB-F from Tokyo Measuring Instruments Lab, whereas the accelerometers were the uni-axial 352C33 from PCB Piezotronics. The PZT patch used as actuator was the P-876.A12 DuraAct from PI Ceramic. The module used to create the voltage signal to feed the patch was the NI-9262. Figure 6 shows all the labelled on-board sensors placed on the top surface of the disk and the PZT actuator placed on the bottom face of the disk.

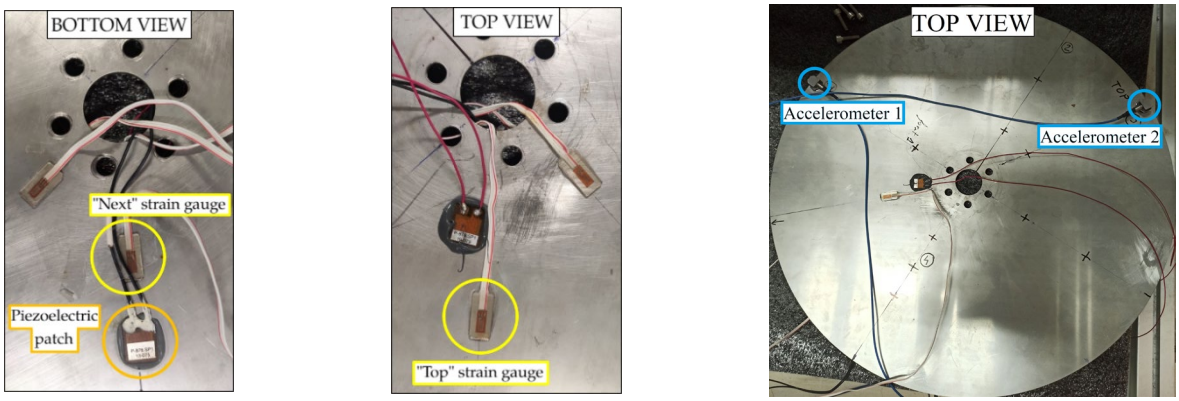

Figure 6. Experimental setup of the onboard sensors and actuators placed on the bottom of the rotating disk (left) and on the top of the disk (centre and right).

The PZT patch was excited with a chirp signal with a range from 0 to 150 Hz and the corresponding acceleration and strain responses were measured with a sampling rate of 5120 Hz, giving as a result the experimental FRFs shown in Figure 7 for the particular case of the disk in air.

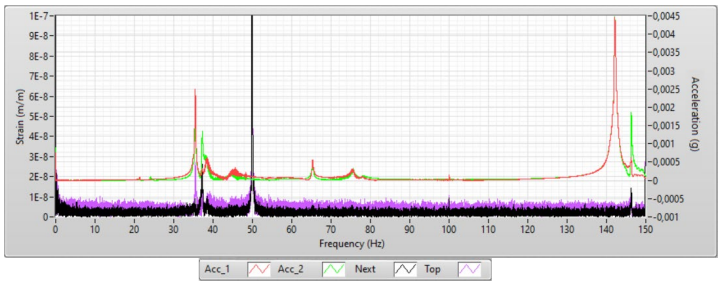

Figure 7. Experimental FRFs of the system obtained with a chirp sweeping from 0 to 150 Hz in air (red and green lines correspond to vibrations and black and purple lines to strains).

Comparing the accuracy of the FRFs obtained from the accelerometers (red and green lines) and from the strain gauges (black and purple lines), it can be seen that the level of excitation of the disk was not enough to achieve an accurate strain response at any natural frequency. Additionally, a peak on the strain response can be seen at 50 Hz due to electrical noise. As a consequence, for the particular case of our test rig, it was decided to only take into consideration the experimental FRFs obtained with the accelerometers and study an alternative way to obtain a FRF for the strains to validate the methodology.

Repeating the same procedure with the disk submerged 115 mm below the water free surface level, the experimental FRFs represented with grey lines in Figure 8 were obtained from both accelerometers. From them, the plant models were identified as shown with the red lines in the same figure. The plant models present different orders to capture the most significant peaks and valleys of the FRFs.

The obtained orders for the models are 12 for the case in air and 14 for the case in water. These orders could not be reduced more, as some significant dynamics of the system could have been lost otherwise.

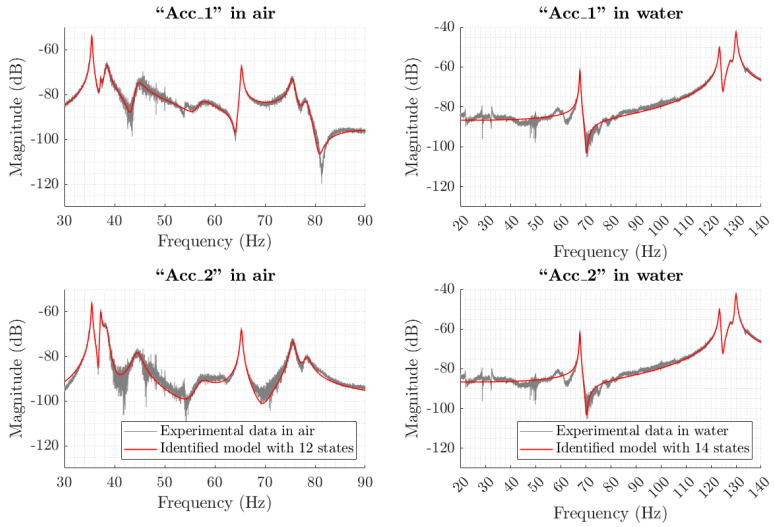

Figure 8. Identified models from the experimental FRFs obtained in air (left) and water (right).

4. Numerical setup

The FRFs of the strain response have been alternatively obtained using a finite element model defined in ANSYS® software and solved through an acoustic-structural coupled harmonic simulation, where the added mass effects induced by the surrounding water have been considered. As presented in Figure 9 (left and center), the model includes the geometry of the shaft, the disk, the onboard PZT actuator and the two unidirectional strain gauges. The created mesh has a total of 353,947 nodes and 220,936 mesh elements.

To setup the harmonic analysis, all the solid parts have been grouped as a "Physic Region", whereas the fluid zones representing the tank of water have been defined as an "Acoustic Region". Additionally, all the faces of the solid that are in contact with the surrounding fluid have been defined as the "Fluid Solid Interface". By using the PiezoAndMems ANSYS® extension [12], the piezoelectric characteristics of the PZT patch have been considered in the simulation and the frequency-varying chirp voltage signal has been applied between both layers of the patch [13]. Finally, the faces of the shaft that are in contact with the bearings have been fixed. Figure 9 (right) shows all the aforementioned boundary conditions set in the harmonic analysis.

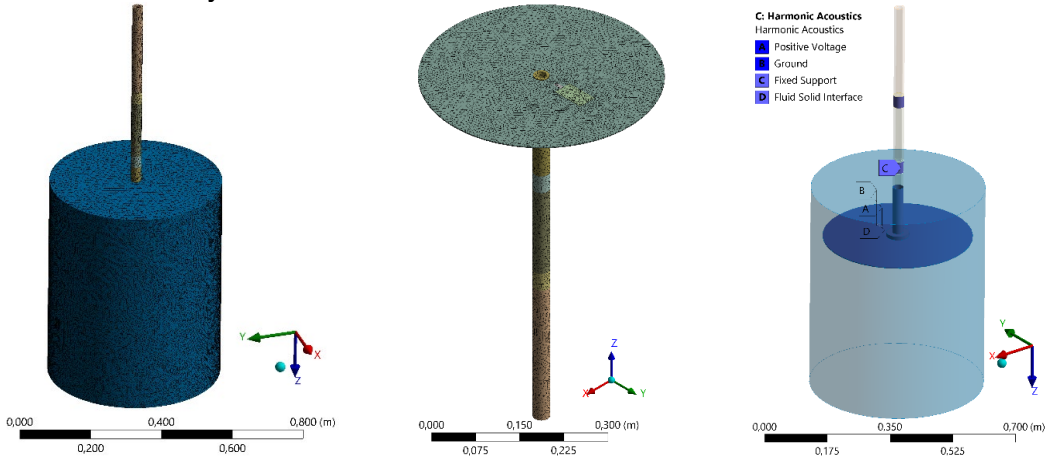

Figure 9. Geometry of the system to model the disk in water with the tank (left), without the tank (centre) and its corresponding boundary conditions (right).

The FRFs shown in Figure 10 have been obtained for a sweeping range from 20 to 325 Hz and setting a typical damping ratio of 2% to the solids. In this case, after identifying the plant models from these FRFs, the model orders have been reduced to end up with only 8 states for the disk in air and 12 in water.

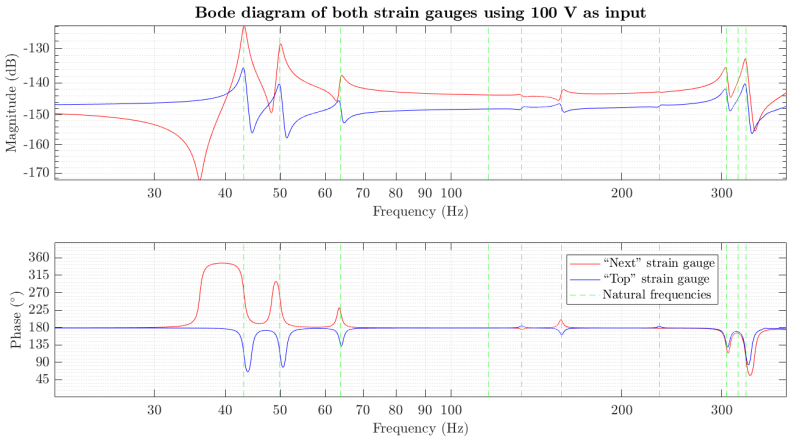

Figure 10. Bode diagram of the identified model of the strain gauges using numerical simulation.

5. Results

With only one PZT control actuation it is only possible to control one response from one sensor mounted on the disk, so the controllers have been designed to reduce only the vibration of the "Next" strain gauge or the "Acc_1" accelerometer. The other two sensors have only been used to ensure the stability and convergence of the control strategy.

5.1. Control approach 1. LQG controller

The tuned LQG controller is able to reduce the strain and the acceleration fluctuations caused by the excitation of a given natural frequency. Figure 11 shows the induced strain without control (black line) and the same strain with the LQG controller (red line) achieved by applying the computed voltage (blue line) to the PZT patch. Even though the only output that is minimized is the strain measured by the "Next" strain gauge (first subplot), the amplitude of the vibrations measured with the "Top" strain gauge (second subplot) also decreases, as the red line shows lower amplitudes than the black line for both sensors and for both air (left) and water (right).

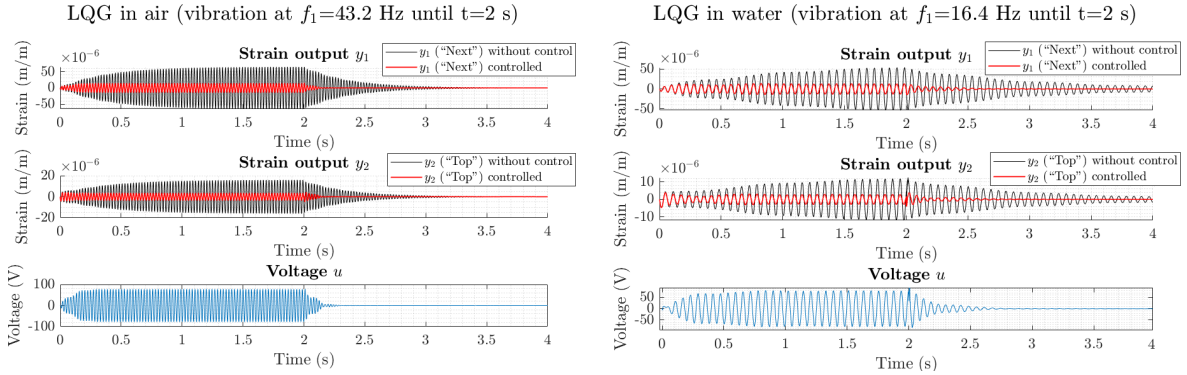

Figure 11. Effect on the strain of the LQG controller in air (left) and in water (right).

The performance of the same LQG controller but with the acceleration as the feedback variable can be seen in Figure 12 (left) for the disk in air and in Figure 12 (right) for the disk submerged in water. This controller is also able to reduce the amplitude of the vibrations, as the red line of the controlled system has less amplitude than the black line of the uncontrolled system.

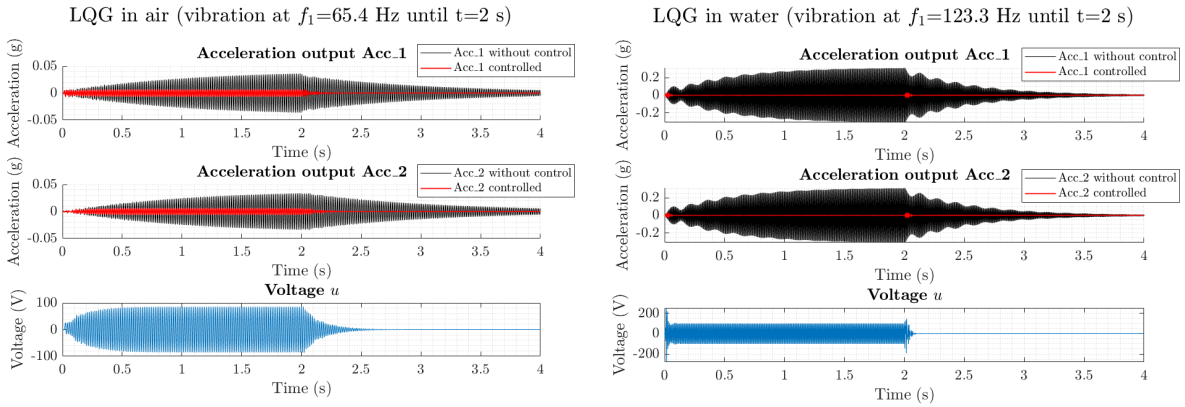

Figure 12. Effect on the acceleration of the LQG controller in air (left) and in water (right).

5.2. Control approach 2. H_∞ controller

The results obtained with the tuned H_∞ controller are presented in Figure 13, where it can be seen that the controlled system (red line) presents significantly lower strain amplitudes than the uncontrolled system (black line) both in air and in water.

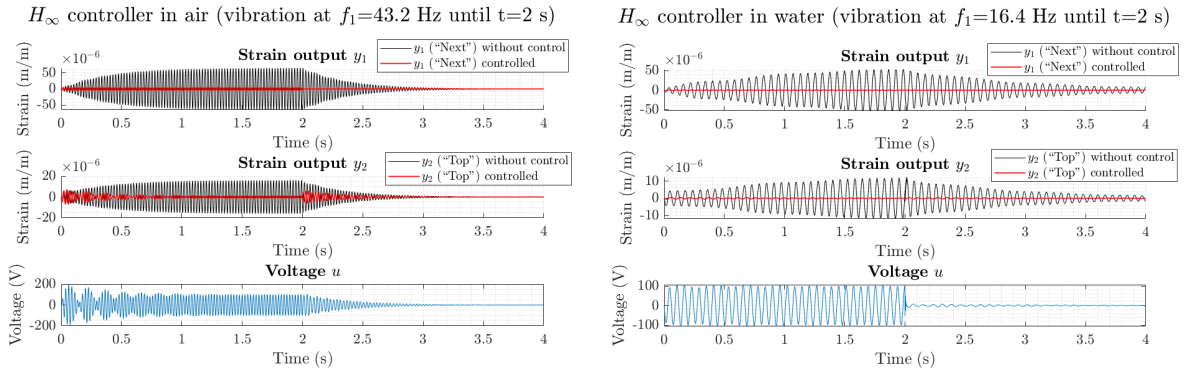

Figure 13. Effect on the strain of the H_∞ controller in air (left) and in water (right).

On the other hand, Figure 14 shows the reduction of the amplitude of the vibration measured in air and in water by the accelerometers "Acc_1" and "Acc_2", being the reduction effects more significant in air.

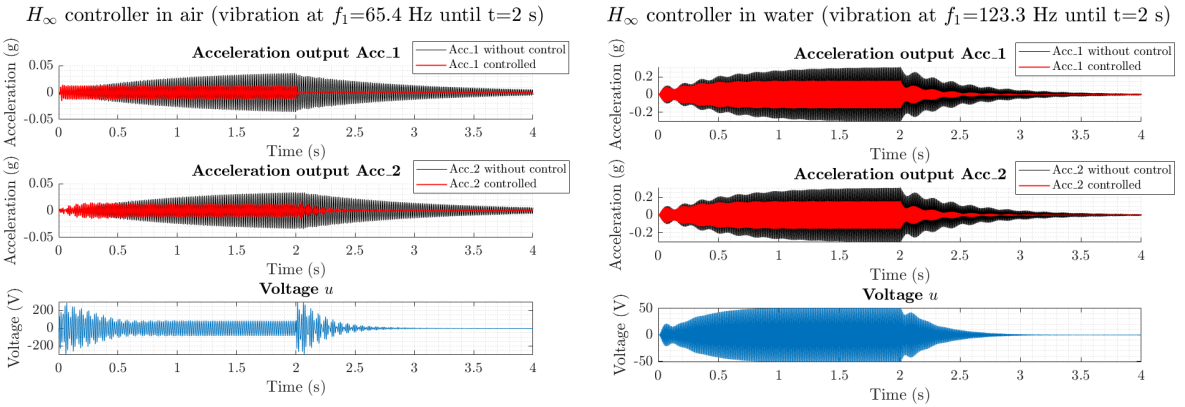

Figure 14. Effect on the acceleration of the H_∞ controller in air (left) and in water (right).

5.3. Comparison of the different controllers

The overall performance of each control approach can be quantified from the reduction percentage of the calculated Root Mean Square (RMS) value of the outputs presented in Table 1.

Table 1. Reduction percentages of RMS levels for each control approach in air and in water.

Output	Controller	Scenario	Vibration freq.	RMS without control	RMS with control	% reduction
Strain (m/m)	LQG	Air	43.2 Hz	$3.1 \cdot 10^{-5}$	$7.4 \cdot 10^{-6}$	76 %
		Water	16.4 Hz	$2.5 \cdot 10^{-5}$	$7.0 \cdot 10^{-6}$	72 %
	H_∞	Air	43.2 Hz	$3.1 \cdot 10^{-5}$	$2.8 \cdot 10^{-6}$	91 %
		Water	16.4 Hz	$2.4 \cdot 10^{-5}$	$3.1 \cdot 10^{-7}$	99 %
Acceleration (g)	LQG	Air	65.4 Hz	$1.6 \cdot 10^{-2}$	$3.6 \cdot 10^{-3}$	78 %
		Water	123.3 Hz	$1.4 \cdot 10^{-1}$	$2.4 \cdot 10^{-3}$	98 %
	H_∞	Air	65.4 Hz	$1.6 \cdot 10^{-2}$	$6.7 \cdot 10^{-3}$	59 %
		Water	123.3 Hz	$1.5 \cdot 10^{-1}$	$8.0 \cdot 10^{-2}$	46 %

The strain responses obtained with the excitation of the same mode of vibration at 43.2 Hz in air and at 16.4 Hz in water have been compared, the latter value being lower due to the water added mass effect. The percent reduction of strain with each control approach is approximately the same in air or in water, being the reduction with the H_∞ controller slightly higher than with the LQG controller.

The acceleration responses have not been evaluated for the natural frequency with the same mode shape in air and in water because the FRFs obtained in water do not capture the lowest modes. In Figure 8 it can be clearly seen how the damping of the system in water reduces the gains of the first natural frequencies. Thus, the identified model only captures the dynamics of high frequency modes with higher gains and it is not able to model the first mode shapes that are clearly identified in air. In spite of the fact of comparing different modes in air and water, it can be seen how the LQG controller obtains a higher percent reduction of accelerations than the H_∞ controller both in air and in water.

To sum up, it is demonstrated that the control performance is strongly dependent on the type of FRF used to model the plant and the method used to obtain it, whether numerical or experimental.

6. Conclusions

The present work has simulated the performance of two types of active controllers to reduce structural vibrations based on models identified from numerically and experimentally obtained FRFs of the system. The FRFs for strains have been numerically obtained using acoustic-structural simulations, whereas the FRFs for accelerations have been experimentally obtained using modal tests.

Comparing the LQG controller with the H_∞ optimal controller, it has been observed that both are able to reduce vibrations and strains when the disk vibrates at a certain natural frequency in air or submerged in water. However, the reduction of strain is higher using the H_∞ optimal controller in air/water, whereas the reduction of acceleration is higher using the LQG controller in air/water.

As future work it is planned to implement both controllers to validate which one gives the best performance in air and in water. For that, a series of experimental verifications of the present simulated results will be carried out in the actual disk using a real-time embedded system. However, it has to be considered that the LQG controller might be more prone to errors due to the uncertainties induced by the parameters estimated with design of the observer. On the other hand, the H_∞ controller might be more robust, as it does not need any extra parameters to define the observer, which is implicit to its optimization design.

Acknowledgements

This project has received funding from the European Union's Horizon 2020 research and innovation program under grant agreement No 814958.

References

[1] *Active Flow Control System for Improving Hydraulic Turbine Performances at off-design Operation.* Available online: https://afc4hydro.eu/ (accessed on 22 February 2022).
[2] Ma R, Bi K and Hao H 2021 Inerter-based structural vibration control: A state-of-the-art review *EngStruct* **243** p 112655, https://doi.org/10.1016/j.engstruct.2021.112655.
[3] Lu Z, Wang Z, Zhou Y and Lu X 2018 Nonlinear dissipative devices in structural vibration control: A review, *J. Sound Vib.* **423** pp 18-49 https://doi.org/10.1016/j.jsv.2018.02.052.
[4] Yu W and Thenozhi S 2016 *Active Structural Control. In: Active Structural Control with Stable Fuzzy PID Techniques*. SpringerBriefs in Applied Sciences and Technology. Springer, Cham. https://doi.org/10.1007/978-3-319-28025-7_2
[5] Kamel M A, Ibrahim K and El-Makarem A 2019 Vibration control of smart cantilever beam using finite element method *Alex. Eng. J.* **58 (2)** pp 591-601, https://doi.org/10.1016/j.aej.2019.05.009.
[6] Khot S and Yelve NP 2011 Modeling and response analysis of dynamic systems by using ansys and matlab *J. Vib. Control* **17** pp 953-8, https://doi.org/10.1177/1077546310377913.
[7] Bagheri S, Jafarov T, Freidovich L and Sepehri N 2016 Beneficially combining LQR and PID to control longitudinal dynamics of a SmartFly UAV *Proc. Int. Conf. on Electronics and Mobile Communication (IEMCON)*, pp 1-6 https://doi.org/10.1109/IEMCON.2016.7746309 .
[8] Zheng Q, Richter H and Gao Z 2013 On active vibration suppression of a piezoelectric beam *Proc. American Control Conf.* pp 6613-8. https://doi.org/10.1109/ACC.2013.6580877
[9] MathWorks, "*Linear-Quadratic-Gaussian (LQG) design*". Available online: https://de.mathworks.com/help/control/ref/ss.lqg.html (accessed on November 2021).
[10] Skogestad S and Postlethwaite I 2001 *Multivariable Feedback Control: Analysis and Design* (New York: John Wiley & Sons. Inc.)
[11] Min K-W, Chung L, Joo S-J and Kim J 2005 Design of Frequency-Dependent Weighting Functions for H2 Control of Seismic-Excited Structures *J. Vib. Control* **11** pp 137-57. https://doi.org/10.1177/1077546305047761 .
[12] ANSYS inc., "*Piezo and mems v2020.1*". Available online: https://catalog.ansys.com/product/5faee26d7f1bd0415ca6a3dc/piezo-and-mems
[13] Pernod L, Lossouarn B, Astolfi J-A and Deü J-F 2021 Vibration damping of marine lifting surfaces with resonant piezoelectric shunts *J. Sound Vib.* **496** p 115921 https://doi.org/10.1016/j.jsv.2020.115921